Contribution from the Department of Chemistry, University of Houston, Houston, Texas 77004, and Isotope Department, The Weizmann Institute of Science, 76100 Rehovot, Israel

Electrochemistry of Nickel(II) Porphyrins and Chlorins

D. CHANG,[1a] T. MALINSKI,[1a] A. ULMAN,[1b] and K. M. KADISH*[1a]

Received June 23, 1983

The electron-transfer mechanisms of five nickel(II) porphyrins and a nickel(II) chlorin were investigated in nonaqueous media. The potentials for oxidation or reduction were monitored by cyclic voltammetry in up to 11 solvents containing either TBAP or TBA(PF_6) as supporting electrolyte. ESR, IR, and electronic absorption spectroscopy were used to monitor the reaction products at both high and low temperature, and these data were used to postulate a reaction mechanism for each of the six investigated complexes. Three difference oxidation mechanisms were found to occur depending upon the nature of the porphyrin or chlorin ring system. In contrast, all of the complexes were reduced by a similar mechanism, which involved formation of anion radicals. Unexpectedly, the three investigated tetraalkylporphyrins showed no evidence for Ni(III) formation as is the case for unsubstituted (TPP)Ni.

Introduction

The electrooxidation–electroreduction of (TPP)Ni[2] has been the subject of several publications over the last 14 years.[3-7] Wolberg and Manassen[3,4] first reported that (TPP)Ni gave two closely overlapping one-electron oxidation steps in benzonitrile. The first of these steps was characterized by ESR as producing $[(TPP)Ni^{III}]^+$, which gradually decayed via internal electron transfer to yield $[(TPP)Ni^{II}]^{+\cdot}$. The product of the second oxidation was assigned as the cation radical $[(TPP)Ni^{III}]^{2+\cdot}$. This assignment was based largely on a plot of Fe(II), Co(II), Ni(II), Cu(II), and Zn(II) oxidation potentials vs. the third ionization potential of each metal.

Dolphin et al.[5,6] later reinvestigated this oxidation in CH_2Cl_2 using either TBAP or TBA(PF_6) as supporting electrolyte. In this study the initial one-electron-transfer product was formulated by room-temperature ESR and electronic absorption spectra as a π cation radical, $[(TPP)Ni^{II}]^{+\cdot}$. However, when this green solution was frozen, an internal electron transfer occurred to produce an orange-red solid of $[(TPP)Ni^{III}]^+$. This assignment was supported by a 77 K anisotropic ESR spectrum of $g_\perp = 2.286$, $g_\parallel = 2.086$ and a frozen-CH_2Cl_2 optical spectrum at 110 K, which was quite different from that of the room-temperature spectrum. Further electrolysis of $[(TPP)Ni^{II}]^{+\cdot}$ at potentials anodic of the second oxidation wave was reported to generate a brown solution whose optical spectrum was that of the dication, $[(TPP)Ni^{II}]^{2+}$.

At about the same time as the above studies, Kadish and Morrison[7] reported half-wave potentials for oxidation and reduction of a series of ((*p*-X)TPP)Ni complexes in CH_2Cl_2. Similar to the earlier results,[3,4] (TPP)Ni gave two closely spaced oxidation waves by cyclic voltammetry. As might be expected, these potentials were dependent on the nature of the electron-donating or electron-withdrawing substituent on the porphyrin ring. The magnitude of the substituent effect was not equal for the two oxidations. Consequently, complexes containing electron-withdrawing substituents (such as $COOCH_3$ or NO_2) gave a single two-electron-transfer process, while those with electron-donating groups (such as CH_3 or OCH_3) had negatively shifted potentials such that two, well-separated, single-electron oxidation processes were obtained. Based in large part on the substituent effects of the two electrode processes, the room-temperature mechanism was assigned as an initial oxidation to yield $[((p\text{-}X)TPP)Ni^{II}]^{+\cdot}$ followed by further oxidation to yield $[((p\text{-}X)TPP)Ni^{III}]^{2+\cdot}$.

In this study, cyclic voltammograms of (TPP)Ni were reexamined and the reactions characterized by spectroelectrochemistry, ESR, and IR. The aim of this aspect of the study was to settle the apparent controversy in the literature regarding the site of initial electron abstraction and, at the same time, use these results as a standard for comparison with results for oxidation and reduction of nickel tetraalkylporphyrins and nickel tetramethylchlorin.

These latter derivatives (especially the nickel *meso*-tetramethylporphyrin) offer several advantages over previously investigated model complexes. Of most importance is the fact that there are no aromatic substituents on the ring that can conjugate with the overall π system. Thus, any physical properties of the complex are localized on the metal or the conjugated ring system. In addition, the reduced products do not have any isomers, thus minimizing ambiguities in interpreting and understanding the physical properties of the reduced products. Finally, the relatively small size of the porphyrin (or chlorin) allows extended theoretical calculations (e.g. electron density maps),[8] which are not easily obtained with the larger molecules.

Nickel tetramethylporphyrin, (TMeP)Ni, and nickel tetramethylchlorin, (TMeC)Ni,[9,10] show a dramatic reduction of the aromaticity in the chlorin relative to that in the porphyrin complex, which is accomplished by an extreme nonplanarity of the (TMeC)Ni molecule. Moreover, the structural parameters indicate an asymmetric charge distribution resulting from an intramolecular charge transfer toward the reduced side of the chlorin. A recent carbon-13 NMR study[11] provides support for this idea.

The structures of the seven investigated complexes are shown in Figure 1. Our interest in this study was to see how the redox potentials and electrode mechanisms would vary by: (i) changing the substitutent at the para position of the four phenyl rings, (ii) replacing the phenyl groups with alkyl groups, and (iii) changing the tetraalkylporphyrin (TMeP)Ni to the tetraalkylchlorin (TMeC)Ni. In addition, the effect of

(1) (a) University of Houston. (b) The Weizmann Institute of Science.
(2) Abbreviations: TPP, 5,10,15,20-tetraphenylporphyrin; (TPP)Ni, (5,10,15,20-tetraphenylporphinato)nickel(II); (TMeP)Ni, (5,10,15,20-tetramethylporphinato)nickel(II); (TEtP)Ni, (5,10,15,20-tetraethylporphinato)nickel(II); (TPrP)Ni, (5,10,15,20-tetrapropylporphinato)nickel(II); (TMeC)Ni, (5,10,15,20-tetramethylchlorinato)nickel(II); OEP, 2,3,7,8,12,13,17,18-octaethylporphyrin.
(3) Wolberg, A.; Manassen, J. *Inorg. Chem.* **1970**, *9*, 2365.
(4) Wolberg, A.; Manassen, J. *J. Am. Chem. Soc.* **1970**, *92*, 2982.
(5) Dolphin, D.; Niem, T.; Felton, R. H.; Fajita, S. *J. Am. Chem. Soc.* **1975**, *97*, 5288.
(6) Johnson, E. E.; Niem, T.; Dolphin, D. *Can. J. Chem.* **1978**, *56*, 1381.
(7) Kadish, K. M.; Morrison, M. M. *Inorg. Chem.* **1976**, *15*, 980.
(8) Ibers, J. A. "Abstracts of Papers"; 185th National Meeting of the American Chemical Society, Seattle, WA, April 1983; American Chemical Society: Washington, DC, 1983; INOR 211.
(9) Ulman, A.; Gallucci, J.; Fisher, D.; Ibers, J. A. *J. Am. Chem. Soc.* **1981**, *102*, 6852.
(10) Gallucci, J.; Ibers, J. A.; Swepston. *Acta Crystallogr., Sect. B: Struct. Crystallogr. Cryst. Chem.* **1982**, *B38*, 2134.
(11) Ulman, A. *Org. Magn. Reson.*, in press.

0020-1669/84/1323-0817$01.50/0

Table I. Half-Wave Potentials for Various Ni(II) Porphyrins in CH_2Cl_2 with 0.1 M TBAP or TBA(PF_6) (Scan Rate 0.1 V/s)

	$E_{1/2}$, V (vs. SCE)						$\Delta E_{1/2}$, V			
	Red		Ox(1)		Ox(2)		Ox(1) − Red(1)		Ox(2) − Ox(1)	
complex	TBAP	TBA(PF_6)	TBAP	TBA(PF_6)	TBAP	TBA(PF_6)	TBAP	TBA(PF_6)	TBAP	TBA(PF_6)
((*p*-Cl)TPP)Ni	−1.18	−1.26	1.13[b]	1.10	1.13[b]	1.34	2.31	2.37	0.00[b]	0.24
(TPP)Ni	−1.28	−1.31	1.05	1.01	1.17	1.31	2.33	2.32	0.12	0.30
(TMeP)Ni	−1.36	−1.40	0.83	0.80	1.15	1.26	2.19	2.20	0.32	0.46
(TEtP)Ni	−1.39	−1.45	0.85	0.81	1.15	1.26	2.24	2.26	0.30	0.45
(TPrP)Ni	−1.41	−1.45	0.85	0.81	1.15	1.26	2.26	2.26	0.30	0.45
((*p*-Et_2N)TPP)Ni[a]	−1.36	−1.43	0.63	0.56	1.11	1.07	1.99	1.99	0.48	0.51
(TMeC)Ni	−1.34	−1.39	0.62	0.58	0.97	1.01	1.96	1.97	0.35	0.43

[a] A third oxidation wave was also observed. This wave was not well-defined with TBAP as supporting electrolyte; however, when TBA(PF_6) was used, a well-defined electrochemically reversible couple centered at 1.33 V was obtained (Figure 2d). [b] Potentials of Ox(1) and Ox(2) are identical, yielding an overall two-electron transfer.

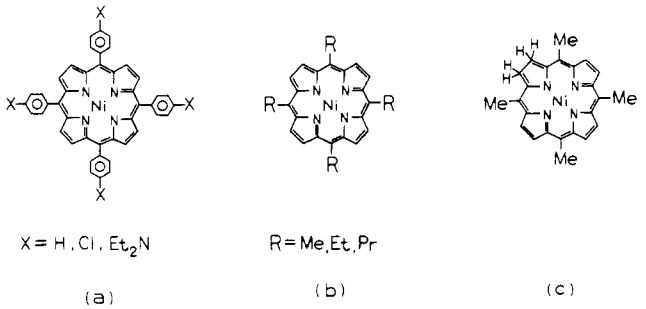

Figure 1. Structural formulas of various PNi^{II} complexes, where P is (a) para-substituted tetraphenylporphyrin, (b) tetraalkylporphyrin, and (c) tetramethylchlorin.

counterion and solvent on the redox processes was investigated by using 11 different nonaqueous solvents with both tetrabutylammonium perchlorate and tetrabutylammonium hexafluorophosphate as supporting electrolyte.

Experimental Section

Reagents. (Tetraphenylporphinato)nickel(II), (TPP)Ni, and its para-substituted derivatives, ((*p*-Cl)TPP)Ni and ((*p*-Et_2N)TPP)Ni, were synthesized by the method of Adler.[12] Meso-substituted tetramethylchlorin and the tetraalkylporphyrin complexes of nickel (TMeC)Ni and (TRP)Ni (where R = Me, Et, Pr) were synthesized by the method of Ulman et al.[9,13] Eleven different nonaqueous solvents were used in this study. These included dichloroethane ($EtCl_2$), methylene chloride (CH_2Cl_2), nitromethane (CH_3NO_2), benzonitrile (C_6H_5CN), acetonitrile (CH_3CN), acetone ($(CH_3)_2CO$), tetrahydrofuran (THF), dimethylformamide (DMF), dimethylacetamide (DMA), dimethyl sulfoxide (Me_2SO), and pyridine (py). The method of purification and source of these solvents are given in a previous publication.[14] For all electrochemical experiments, the solvents contained 0.1 M supporting electrolyte. Two supporting electrolytes were utilized: tetrabutylammonium perchlorate (TBAP) and tetrabutylammonium hexafluorophosphate (TBA(PF_6)). Both were recrystallized and dried in vacuo prior to use.

Instrumentation. Cyclic voltammetric measurements were made by using a conventional three-electrode configuration and an IBM Model EC 225 voltammetric analyzer. A platinum button served as a working electrode and a platinum wire as a counterelectrode for conventional cyclic voltammetric measurements. A saturated calomel electrode (SCE), which was separated from the bulk of the solution by a fritted-glass disk, was used as the reference electrode. Measurements of electron-transfer rate constants were obtained by the cyclic voltammetric technique of Nicholson[15] using positive feedback (which was built into each potentiostat) and a Luggin capillary. In addition, low but exact porphyrin concentrations (less than 0.5 mM) were utilized in order to minimize the peak currents and thus the *iR* loss.

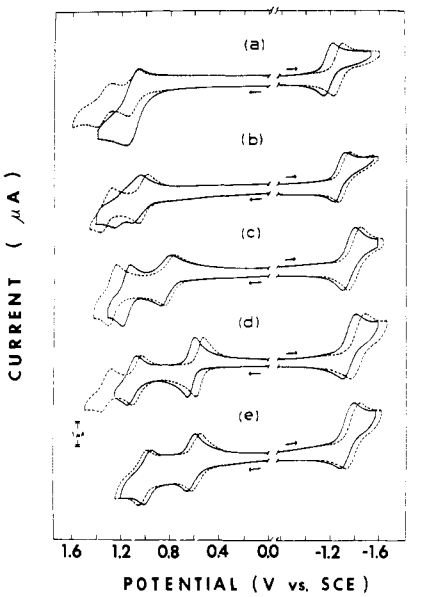

Figure 2. Cyclic voltammograms of (a) ((*p*-Cl)TPP)Ni, (b) (TPP)Ni, (c) (TMeP)Ni, (d) ((*p*-Et_2N)TPP)Ni, and (e) (TMeC)Ni in CH_2Cl_2 with 0.1 M TBAP (—) and 0.1 M TBA(PF_6) (---) (scan rate 0.1 V/s).

For controlled-potential coulometry and controlled-potential electrolysis, a Princeton Applied Research Model 173 potentiostat was used to control the potential. Integration of the current–time curve was achieved by means of a PAR Model 179 integrator. A three-electrode configuration was used, consisting of a Pt wire mesh working electrode, a Pt-wire counterelectrode separated from the main solution by a glass frit, and an SCE as the reference electrode. Spectroelectrochemistry was performed in a bulk cell that followed the design of Fajer et al.,[16] and had an optical path length of 0.19 cm. This spectroelectrochemical cell was coupled with a Tracor Northern 1710 optical spectrometer/multichannel analyzer to obtain time-resolved spectra.

ESR spectra at room temperature as well as at 77 K were recorded on an IBM Model ER 100D spectrometer, equipped with an ER 040-X microwave bridge and an ER 080 power supply. The cavity was cooled by a stream of liquid nitrogen, which was constantly passed through the variable-temperature insert. Samples were introduced into the cavity in a sealed quartz tube immersed in a liquid-nitrogen Dewar. The *g* values were measured relative to diphenylpicrylhydrazyl (DPPH) ($g = 2.0036 \pm 0.0003$). IR experiments were performed on a Beckman 4250 infrared spectrophotometer with a thin-layer cell of path length 0.01 cm.

Results and Discussion

Cyclic voltammograms of five representative compounds in CH_2Cl_2 containing either TBAP or TBA(PF_6) as supporting electrolyte are shown in Figure 2, and a summary of the

(12) Adler, A. D.; Longo, F. R.; Kampas, F.; Kim, J. *J. Inorg. Nucl. Chem.* **1970**, *32*, 2443.
(13) Ulman, A.; Fisher, D.; Ibers, J. A. *J. Heterocycl. Chem.* **1982**, *19*, 409.
(14) Kadish, K. M.; Chang, D. *Inorg. Chem.* **1982**, *21*, 3614.
(15) Nicholson, R. S. *Anal. Chem.* **1965**, *37*, 1351.
(16) Fajer, J.; Borg, D. C.; Forman, A.; Dolphin, D.; Felton, R. H. *J. Am. Chem. Soc.* **1970**, *92*, 3451.

reversible half-wave potentials for the seven investigated complexes is listed in Table I. The complexes in Table I are listed in order of increasing porphyrin (or chlorin) ring basicity so that trends in potential can be most easily observed and characterized. Six of the seven compounds underwent a single reduction (between −1.26 and −1.45 V) and two oxidations (between 0.56 and 1.10 V for Ox(1) and between 1.01 and 1.34 V for Ox(2)). A seventh compound, ((*p*-Et_2N)TPP)Ni, had a fourth wave at $E_{1/2}$ = 1.33 V when TBA(PF_6) was used as supporting electrolyte.

As illustrated in Figure 2, potentials for the first reduction and the second oxidation varied by up to 330 mV with changes in porphyrin (or chlorin) ring basicity. In contrast, half-wave potentials for the first oxidation were the most sensitive to ring basicity and shifted by 510 mV on going from ((*p*-Cl)TPP)Ni to ((*p*-Et_2N)TPP)Ni. Earlier electrochemical studies of (TPP)Ni showed that the difference between the first and second oxidation (Ox(2) − Ox(1)) increased by 120 mV on changing the supporting electrolyte from TBAP to TBA(PF_6).[6] This increase was also observed in this study for each of the seven complexes and amounted to between 30 and 210 mV, depending upon the complex. This shift of potential is due to differences in adsorption characteristics of the complexes between the two supporting electrolyte systems and, in all cases, results in a positive shift of the second oxidation potential with use of TBA(PF_6). Potentials for the single reduction process are negatively shifted when TBA(PF_6) (Figure 2, dashed line) is used instead of TBAP (Figure 2, solid line). At the same time, however, the potential differences between $E_{1/2}$(Ox(1)) and $E_{1/2}$(Red(1)) remained virtually identical between the two systems. This is shown in Table I and indicates that the absolute potential difference between the HOMO and the LUMO is unaffected by changes in supporting electrolyte.

Controlled-potential electrolysis was carried out after each reaction and an overall oxidation–reduction mechanism assigned on the basis of the resulting spectral characterization of the reaction products. These mechanisms are discussed below under four main groups of compounds: (1) the Cl- and H-substituted tetraphenylporphyrins, (2) the tetraalkyl-substituted porphyrins, (3) the diethylamino-substituted tetraphenylporphyrin, and (4) the tetraalkyl-substituted chlorin.

Electrochemistry of (TPP)Ni and ((*p*-Cl)TPP)Ni in CH_2Cl_2. In CH_2Cl_2 with 0.1 M TBAP (TPP)Ni displays two partially overlapping oxidations centered at 1.05 and 1.17 V and a reduction at −1.28 V. When TBA(PF_6) is used as supporting electrolyte, two well-defined oxidations and one reduction are observed at $E_{1/2}$ = 1.01, 1.31, and −1.31 V. These waves are shown in Figure 2b and are consistent with results previously reported under the same experimental condition.[6] In the same solvent, containing 0.1 M TBAP, ((*p*-Cl)TPP)Ni shows only one oxidation (1.13 V) and one reduction (−1.18 V). Controlled-potential coulometry at 1.30 and −1.30 V gave 2.0 ± 0.2 and 1.05 ± 0.05 electrons, respectively. When TBA(PF_6) is used to replace TBAP, two well-defined one-electron oxidations ($E_{1/2}$ = 1.10 and 1.34 V) and one single-electron reduction ($E_{1/2}$ = −1.26 V) are observed (Figure 2a).

Exhaustive electrolysis at potentials anodic of the first oxidation wave for (TPP)Ni (with either TBAP or TBA(PF_6) as supporting electrolyte) and ((*p*-Cl)TPP)Ni (with 0.1 M TBA(PF_6)) produced similar green solutions at room temperature having similar isotropic ESR signals with *g* values of 2.008 and 2.005, respectively. These values are clearly indicative of a π cation radical.[3-6,17,18] The infrared spectra

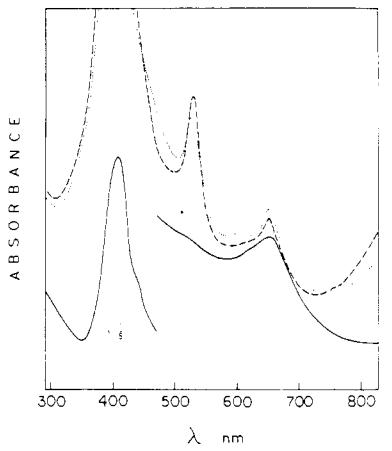

Figure 3. Optical absorption spectra, in CH_2Cl_2, of [((*p*-Cl)TPP)Ni^{II}]$^+$·[PF_6]$^-$ at room temperature (—) and at 130 K (- - -) and [(TPP)Ni^{III}]$^+ClO_4^-$ at 130 K (···).

Scheme I

$$[PNi^{III}]^+ \overset{-\Delta}{\rightleftharpoons} [PNi^{II}]^+\cdot \overset{e^-}{\rightleftharpoons} PNi^{II} \overset{e^-}{\rightleftharpoons} [PNi^{II}]^-\cdot$$

$$e^- \downarrow\uparrow$$

$$[PNi^{III}]^{2+}\cdot$$

of [(TPP)Ni]$^+$· had an IR band at 1279 cm^{-1} while [(*p*-Cl)-TPP)Ni]$^+$· had a band at 1280 cm^{-1}. These two bands fall within the region of 1270–1295 cm^{-1}, which is an operational diagnostic criteria[19] for the presence of tetraphenylporphyrin cation radicals.

A dramatic spectral change was observed when the temperature of the radical solutions was lowered below 150 K. This thermal behavior has been observed previously for (TPP)Ni[5,6] and is shown in Figure 3 for ((*p*-Cl)TPP)Ni. The frozen orange-red solid has an intense peak at 530 nm (dashed line) compared to 527 nm for frozen [(TPP)Ni]$^+$· (dotted line). For comparison purposes the spectrum of the green [((*p*-Cl)TPP)Ni^{II}]$^+$· solution at room temperature (solid line) is also included. As seen in the figure, there is a very significant difference in the region near 528 nm, indicating[6] a change in the site of electron abstraction. Further electrolysis of the singly oxidized green solutions at 1.40 V gave ESR-inactive brown solutions at room temperature, and no ESR signals were detected from this solution at any temperature. The spectral changes obtained during controlled-potential oxidations are shown in Figure 4b,c,e,f. As seen in this figure, the spectra of the corresponding green (Figure 4b,e) and brown (Figure 4c,f) solutions in these two systems have almost identical large decreases in the Soret peak and broad absorptions in the range of 550–900 nm and are consistent with the formation of π cation radicals and dications.[4-6,16,18,20-22]

When exhaustive electroreduction was carried out at −1.50 V on a freshly prepared solution of (TPP)Ni in CH_2Cl_2 (0.1 M TBAP), a green solution was obtained, which gave an isotropic room-temperature ESR signal (*g* = 2.007). The spectral changes obtained during this reduction are shown in Figure 4d. At the same time there was a decrease in the intensity of the Soret peak and broad absorptions around 616 and 773 nm, indicating the formation of a π anion radical.

(17) Fuhrhop, J.-H.; Manzerall, D. *J. Am. Chem. Soc.* **1969**, *91*, 4174.
(18) Felton, R. H.; Owen, G. S.; Dolphin, D.; Forman, A.; Borg, D. C.; Fajer, J.; *Ann. N.Y. Acad. Sci.* **1973**, *206*, 504.
(19) Shimomura, E. T.; Phillippi, M. A.; Goff, H. M. *J. Am. Chem. Soc.* **1981**, *103*, 6778.
(20) Brown, G. M.; Hopf, F. R.; Ferguson, J. A.; Meyer, T. J.; Whitten, D. G. *J. Am. Chem. Soc.* **1973**, *95*, 5939.
(21) Malinski, T.; Chang, D.; Bottomley, L. A.; Kadish, K. M. *Inorg. Chem.* **1982**, *21*, 4248.
(22) Fuhrhop, J.-H.; Kadish, K. M.; Davis, D. G. *J. Am. Chem. Soc.* **1973**, *95*, 5140.

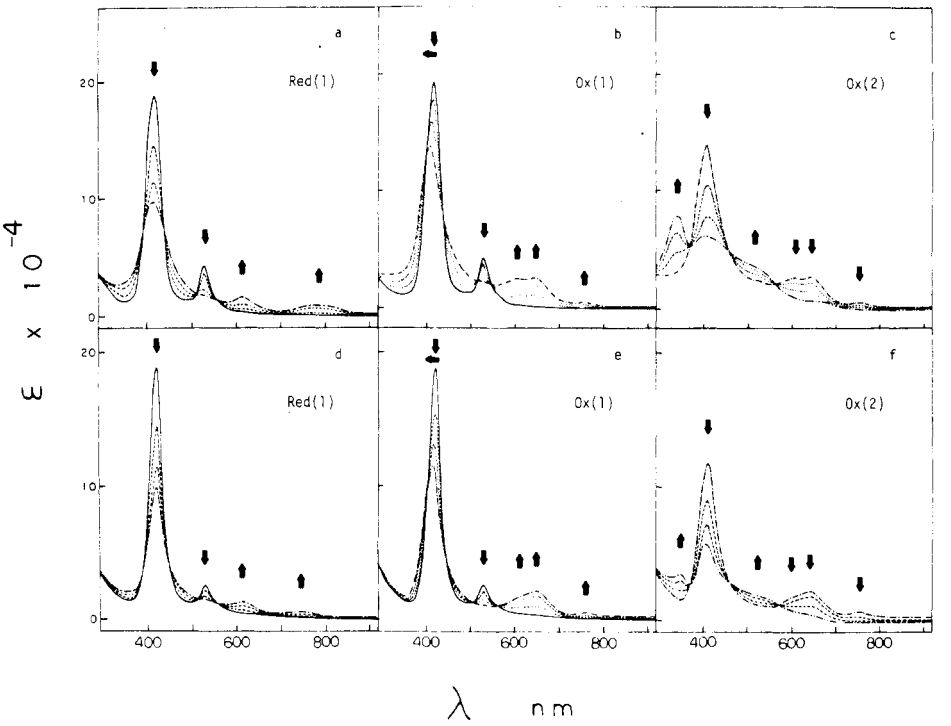

Figure 4. Time-resolved electronic absorption spectra obtained during exhaustive electrolysis of (a–c) ((*p*-Cl)TPP)Ni and (d–f) (TPP)Ni in CH_2Cl_2 (0.1 M TBAP).

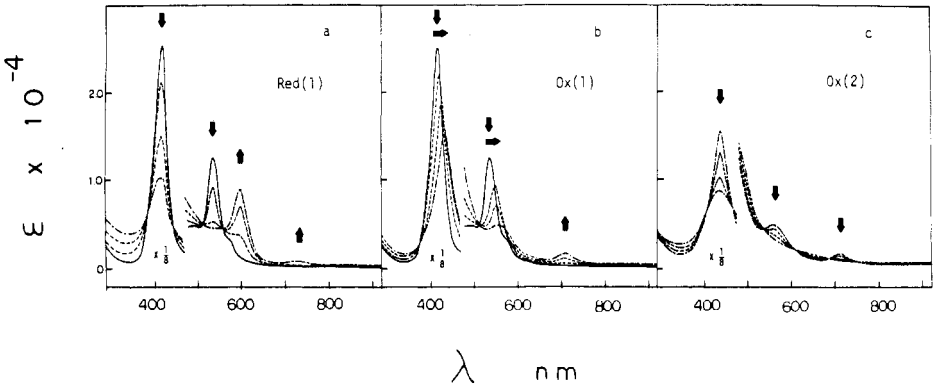

Figure 5. Time-resolved electronic absorption spectra obtained during exhaustive electrolysis of (TMeP)Ni in CH_2Cl_2 (0.1 M TBAP).

When ((*p*-Cl)TPP)Ni was reduced in a similar manner, almost identical spectral changes were observed (Figure 4a).

In summary the electrochemical and spectral data of (TPP)Ni and ((*p*-X)TPP)Ni oxidation and reduction products are consistent with previous results in the literature for (TPP)Ni. There is a great similarity between these two complexes, and the overall oxidation–reduction scheme may be presented as shown in Scheme I, where P = TPP or (*p*-Cl)TPP.

The potentials for the above electrode reactions are summarized in Table I for both TBAP and $TBA(PF_6)$ supporting electrolyte. As seen in this table, the differences in potential ($\Delta E_{1/2}$) between the first oxidation, Ox(1), and the first reduction, Red(1), equals 2.31–2.37 V (depending on supporting electrolyte) for ((*p*-Cl)TPP)Ni and 2.32–2.33 V for (TPP)Ni. These values fall within the range of 2.25 ± 0.15 V, which has often been used to predict that both the oxidation and reduction are centered on the conjugated porphyrin ring.[22] It is also interesting to note that when $TBA(PF_6)$ was used as supporting electrolyte, the potential difference between the two one-electron oxidation waves, $\Delta E_{1/2}$(Ox(2) – Ox(1), was 0.24 V for ((*p*-Cl)TPP)Ni and 0.30 V for (TPP)Ni. Both of these values are within the range of 0.29 ± 0.05 V found for a series of metalloporphyrins where both oxidations are known to be at the conjugated π systems.[22]

Electrochemistry of (TRP)Ni^{II}, Where R = Me, Et, Pr. All three (TRP)Ni^{II} complexes gave two oxidations and one reduction with either 0.1 M TBAP or 0.1 M $TBA(PF_6)$ as supporting electrolyte. The half-wave potentials for these reactions are listed in Table I, and a typical cyclic voltammogram for one of the complexes, (TMeP)Ni, is shown in Figure 2c. As seen in Table I, there is no significant difference in potentials between the three complexes. Although the electron-donating ability of the alkyl group increases on going from methyl to ethyl to propyl, this is not completely reflected in the half-wave potentials. There is virtually no change in the oxidation potentials, but a 50-mV shift does appear in the reduction potentials, which are found at −1.36, −1.39, and −1.41 V, respectively. On the other hand, the maximum potential shift for (TRP)Ni with respect to (TPP)Ni is 200–220 mV for the oxidations but only 130 mV for the reductions. Also, when TBAP was used as supporting electrolyte, the peak separations of $\Delta E_{1/2}$(Ox(1) – Red(1)) and $\Delta E_{1/2}$(Ox(2) – Ox(1)) for (TRP)Ni ranged from 2.19 to 2.26 and 0.30 to 0.32 V, respectively. These values fall within the range of 2.25 ± 0.15 and 0.29 ± 0.05 V, suggesting that all reactions of (TRP)Ni are porphyrin ring based.[22]

Controlled-potential electrolysis was performed after each electron transfer, and the associated spectra were recorded.

Table II. Absorption Maxima (nm) and Molar Absorptivities (ϵ) of Various Ni(II) Porphyrins in CH_2Cl_2[a]

	λ_{max}, nm ($\epsilon \times 10^{-4}$)									
	neutral		Red		Ox(1)		Ox(2)	
porphyrin	Soret	Q	Soret	Q	Soret	Q	Soret	Q
((*p*-Cl)TPP)Ni	416 (19.8)	487 (s), 527 (2.54), 558 (sh)	416 (9.93)	521 (s), 612 (1.51), 748 (0.69)	410 (11.7)	605 (sh), 649 (2.38), 752 (0.31)	352 (1.71), 408 (5.32)	535 (sh), 649 (sh)
(TPP)Ni	414 (19.1)	490 (s), 525 (3.73), 555 (sh)	414 (9.95)	522 (1.69), 600 (1.78), 762 (0.99)	410 (13.4)	606 (2.54), 641 (2.61), 750 (0.42)	350 (8.14), 410 (5.42)	512 (3.73), 648 (s)
(TMeP)Ni	418 (18.9)	502 (s), 537 (1.22), 570 (sh)	418 (6.58)	549 (s), 600 (0.55), 722 (s)	431 (12.1)	558 (0.60), 603 (sh), 720 (0.39)	422 (3.15)	
(TEtP)Ni	417 (18.6)	501 (s), 535 (1.13), 572 (sh)	417 (6.76)	540 (s), 601 (0.66), 723 (s)	434 (12.0)	560 (0.57), 607 (sh), 720 (0.39)	423 (4.01)	
(TPrP)Ni	417 (27.8)	502 (s), 536 (1.82), 571 (sh)	418 (6.80)	541 (s), 606 (0.48), 721 (s)	436 (18.9)	564 (0.77), 607 (0.68), 720 (0.49)	427 (7.32)	
((*p*-Et_2N)TPP)Ni	447 (16.8)	542 (3.04), 587 (2.57)	442 (7.44)	545 (2.05), 607 (2.51)	406 (5.46)	492 (11.3), 527 (12.3)	416 (16.4)	490 (s), 528 (3.73)
(TMeC)Ni	421 (14.9)	582 (0.95), 617 (2.30)	417 (3.71)	617 (0.33)	421 (16.8)	539 (1.79), 582 (sh), 754 (0.42)	419 (6.86)	695 (s)

[a] Abbreviations: s, small peak; sh, shoulder peak.

Table III. ESR Data[a] for Various Singly Oxidized Ni(II) Porphyrins in CH_2Cl_2 (0.1 M TBAP)

complex	295 K	77 K		
	g_{av}	g_{av}	$g_\parallel$	$g_\perp$
$[((p\text{-Cl})TPP)Ni^{II}]^{+\cdot}$	2.005	2.220	2.085	2.287
$[(TPP)Ni^{II}]^{+\cdot}$	2.008	2.219	2.090	2.284
$[(TPP)Ni^{II}]^{-\cdot}$	2.007	2.007		
$[(TMeP)Ni^{II}]^{+\cdot}$	2.006	2.007		
$[(TEtP)Ni^{II}]^{+\cdot}$	2.007	2.009		
$[(TPrP)Ni^{II}]^{+\cdot}$	2.010	2.011		
$[((p\text{-}Et_2N)TPP)Ni^{II}]^{+\cdot}$	2.005	2.003		
$[(TMeC)Ni^{II}]^{+\cdot}$	2.005	2.004		

[a] All g values ±0.001.

Scheme II

$$[(TRP)Ni^{II}]^{+\cdot} \overset{e^-}{\rightleftharpoons} (TRP)Ni^{II} \overset{e^-}{\rightleftharpoons} [(TRP)Ni^{II}]^{-\cdot}$$

$$\Big\Updownarrow e^-$$

$$[(TRP)Ni^{II}]^{2+}$$

These spectra are illustrated in Figure 5 and the molar absorptivities of the major peaks summarized in Table II. As might be expected, there were no distinctive differences in the electronic absorption spectra of the three complexes. Both the Soret and Q bands decreased in intensity and shifted to longer wavelengths with the production of a brown-green solution after electrolysis at 1.0 V. At the same time a new band was formed at 720 nm, indicating radical cation formation. The ESR spectra of all three brown-green $[(TRP)Ni^{II}]^{+\cdot}$ solutions showed room-temperature isotropic signals with g values ranging from 2.006 to 2.010 at room temperature. These values are listed in Table III. When the temperature was lowered to 77 K, no color change was observed for the frozen solids, which had similar isotropic ESR signals with g values from 2.007 to 2.011 (Table III). This is unlike the case of (TPP)Ni and ((*p*-Cl)TPP)Ni, which showed a temperature dependent change in the electron-transfer site. Further oxidation of these green-brown solutions at 1.30 V produced a yellow-green solution, whose spectrum (Figure 5c) is similar to that of the π dication $[(TPP)Zn^{II}]^{2+}$ and $[(TPP)Mg^{II}]^{2+}$.[16] No ESR signal was detected at this point.

The optical absorption spectra recorded during reduction of (TMeP)Ni at −1.50 V is shown in Figure 5a. These spectral changes are almost identical for (TEtP)Ni and (TPrP)Ni and similar to those observed during ((*p*-Cl)TPP)Ni and (TPP)Ni reductions (Figure 4a,d), strongly suggesting that the same electron-transfer mechanism (formation of an anion radical) has occurred. Thus, on the basis of the electronic absorption spectra, ESR spectra, and the redox potentials, the mechanism for (TRP)Ni oxidation–reduction may be postulated to occur as shown in Scheme II.

Electrochemistry of ((*p*-Et_2N)TPP)Ni^{II}. Two well-defined oxidations (at $E_{1/2}$ = 0.63 and 1.11 V) and one well-defined reduction (at $E_{1/2}$ = −1.36 V) were observed in solutions of ((*p*-Et_2N)TPP)Ni containing TBAP as supporting electrolyte. In addition, a third ill-defined oxidation wave was observed at ~1.4 V. This third wave was very well defined when TBA(PF_6) was used as supporting electrolyte. This is illustrated by the dashed curve in Figure 2d. The electron-donating Et_2N group on the phenyl ring of (TPP)Ni produces the most basic nickel porphyrin yet investigated and results in a predicted cathodic shift of half-wave potentials with respect to (TPP)Ni. Half-wave potentials for all four reactions of ((*p*-Et_2N)TPP)Ni are summarized in Table I. The magnitude of the potential shift (in TBAP solutions) amounts to 420 mV for the first oxidation and 80 mV for the first reduction and is similar to values observed for ((*p*-Et_2N)TPP)Ru(CO) in the same solvent.[21]

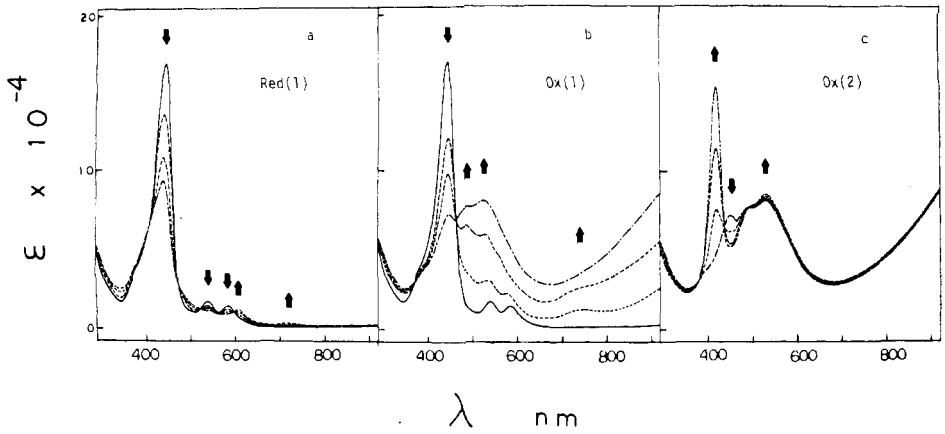

Figure 6. Time-resolved electronic absorption spectra obtained during exhaustive electrolysis of ((*p*-Et_2N)TPP)Ni in CH_2Cl_2 (0.1 M TBAP).

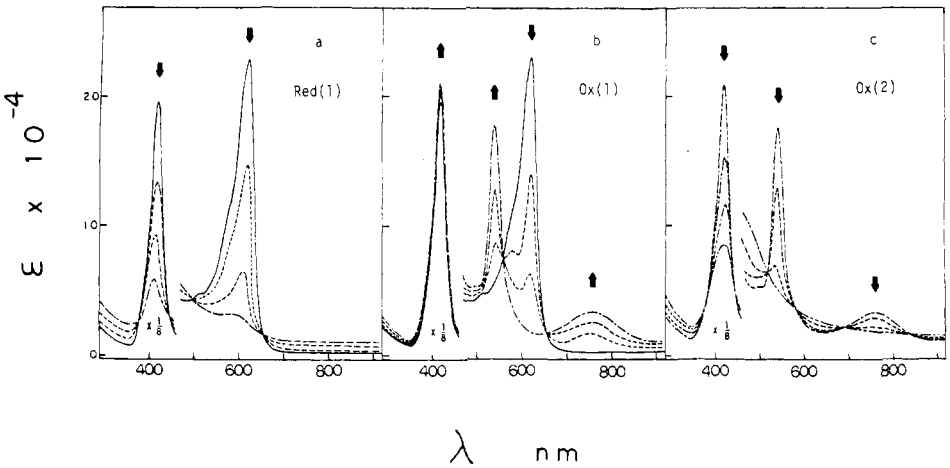

Figure 7. Time-resolved electronic absorption spectra obtained during exhaustive electrolysis of (TMeC)Ni in CH_2Cl_2 (0.1 M TBAP).

Spectral changes recorded during stepwise exhaustive electrolysis of ((*p*-Et_2N)TPP)Ni are shown in Figure 6. Similar spectral changes were obtained with either TBAP or TBA(PF_6) as supporting electrolyte. When the potential was set at 0.85 V, the solution color turned from brown-green to pink, and the final product showed a spectrum with broad absorptions between 450 and 900 nm (Figure 6b). This spectrum is similar to that of the free-base radical $[((p\text{-}Et_2N)TPP)H_2]^{+\cdot}$ (not shown) and suggests the formation of a π cation radical, $[((p\text{-}Et_2N)TPP)Ni^{II}]^{+\cdot}$. The ESR spectrum of this pink solution exhibited a single isotropic signal at g = 2.005 (295 K) or 2.003 (77 K). An IR spectrum of the same solution displayed a band at 1276 cm^{-1}, indicating formation of a cation radical.[19]

Further electrolysis of the pink oxidation product gave a brown solution, which had an intense Soret peak at 416 nm and retained the broad absorption from 450 to 900 nm, with absorption maxima at 484 and 525 nm (Figure 6c). This spectrum is unlike the spectra of other Ni(II) dications (Figures 4c,f, and 5c). It is also different from those of the $[(TPP)Zn]^{2+}$ or $[(OEP)Mg]^{2+}$ dications.[16] The spectrum most closely resembles that of a Ni(III) cation radical. Further support for this assignment comes from the large peak separation between the two oxidations ($\Delta E_{1/2}$ = 0.48–0.51), which deviates substantially from the average value of 0.29 ± 0.05 V reported for two consecutive ring oxidations.[22]

Spectral changes were also recorded during the third oxidation of ((*p*-Et_2)TPP)Ni. The final spectrum (not shown) has a significantly decreased Soret band and broad absorptions between 600 and 900 nm. This spectrum is similar to that observed for a number of metalloporphyrin dications, and therefore the product is considered as a π dication, $[((p\text{-}Et_2N)TPP)Ni^{III}]^{3+}$. Attempts to obtain an ESR spectrum of this product were unsuccessful, because of a poor stability of the highly charged complex. Similar difficulty with the ESR of other Ni(III) porphyrins has been reported in the literature.[3,6] When exhaustive electrolysis of ((*p*-Et_2N)TPP)Ni was carried out at −1.50 V, a green solution was produced. This green solution showed a spectrum (Figure 6a) consistent with that of other Ni(II) π anion radicals (Figures 4a,d, and 5a), indicating the formation of $[((p\text{-}Et_2N)TPP)Ni^{II}]^{-\cdot}$.

Thus, the basis of the above results there appears to be little doubt that the overall oxidation–reduction mechanism of ((*p*-Et_2N)TPP)Ni is as shown in Scheme III.

Electrochemistry of (TMeC)Ni in CH_2Cl_2. Figure 2e illustrates a cyclic voltammogram of (TMeC)Ni in CH_2Cl_2 with both 0.1 M TBAP and TBA(PF_6) as supporting electrolytes. With both supporting electrolytes, a single reduction and two oxidations were observed. Half-wave potentials of these reactions are listed in Table I. There is little change in $E_{1/2}$ for reduction of (TMeC)Ni when compared to that of (TMeP)Ni. In contrast, half-wave potentials for the first oxidation of (TMeC)Ni are negatively shifted by 210–220 mV from those of (TMeP)Ni under the same solution conditions. Similar differences in oxidation potentials have been reported for other metalloporphyrins and metallochlorins. These include (TPP)Zn and (TPC)Zn,[23] (OEP)FeX and (OEC)FeX (where X = Cl^-, OAc^-),[23] and $[(OEP)Fe]_2O$ and $[(OEC)Fe]_2O$.[24]

Controlled-potential electrolysis in CH_2Cl_2 with 0.1 M

(23) Chang, C. K.; Hanson, L. K.; Richardson, P. F.; Young, R.; Fajer, J. *Proc. Natl. Acad. Sci. U.S.A.* **1981**, *78*, 5, 2652.
(24) Stolzenberg, A. M.; Strauss, S. H.; Holm, R. H. *J. Am. Chem. Soc.* **1981**, *103*, 4763.

Scheme III

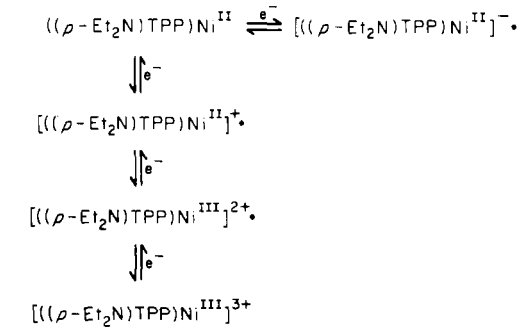

Table IV. Half-Wave Potentials (V vs. SCE and vs. Fc^+/Fc) for the Redox Reactions of $(TPP)Ni^{II}$ in Selected Solvents Containing 0.1 M TBAP (Scan Rate 0.1 V/s)

		Red(1)		Ox(1)		Ox(2)	
solvent	DN[a]	vs. SCE	vs. Fc^+/Fc	vs. SCE	vs. Fc^+/Fc	vs. SCE	vs. Fc^+/Fc
$EtCl_2$	0.0	−1.23	−1.73	1.09	0.59	1.20	0.70
CH_2Cl_2	0.0	−1.28	−1.76	1.05	0.57	1.17	0.69
C_6H_5CN	11.9	−1.26	−1.72	1.02	0.56	1.13	0.67
THF	20.0	−1.20	−1.73	1.08	0.55	1.15	0.62
DMF	26.6	−1.17	−1.64	0.96	0.49	*b*	
py	33.1	−1.21	−1.71	0.69	0.19	1.07	0.57

[a] Gutmann, V. "The Donor-Acceptor Approach to Molecular Interactions"; Plenum Press: New York, 1978. [b] Not observed.

Table V. Half-Wave Potentials (V vs. SCE and vs. Fc^+/Fc) for the Redox Reactions of (TPrP)Ni in Different Solvents Containing 0.1 M TBAP

		Red(1)		Ox(1)		Ox(2)	
solvent	DN[a]	vs. SCE	vs. Fc^+/Fc	vs. SCE	vs. Fc^+/Fc	vs. SCE	vs. Fc^+/Fc
$EtCl_2$	0.0	−1.39	−1.89	0.88	0.38	1.14	0.64
CH_2Cl_2	0.0	−1.41	−1.89	0.85	0.37	1.15	0.67
CH_3NO_2	2.1	*b*		0.75	0.41	0.99	0.65
C_6H_5CN	11.9	−1.43	−1.89	0.87	0.41	1.08	0.62
CH_3CN	14.1	−1.41	−1.81	0.80	0.40	1.23	0.83
$(CH_3)_2CO$	17.0	−1.37	−1.87	0.89	0.39	1.03	0.53
THF	20.0	−1.36	−1.89	0.93	0.40	1.03	0.50
DMF	26.6	−1.37	−1.84	0.82	0.35	1.04	0.57
DMA	27.8	−1.35	−1.85	0.89	0.39	*b*	
Me_2SO	29.8	−1.35	−1.80	0.77	0.32	0.99	0.54
py	33.1	−1.40	−1.90	0.55	0.05	0.82	0.32

[a] Gutmann, V. "The Donor-Acceptor Approach to Molecular Interactions"; Plenum Press: New York, 1978. [b] Not observed.

Table VI. Heterogeneous Electron-Transfer Rate Constants (10^{-2} cm/s) for Redox Reactions of Various Ni(II) Porphyrin Complexes in CH_2Cl_2 (0.1 M TBAP)

complex	Red	Ox(1)	Ox(2)
(TPP)Ni	3.7	1.9	*a*
(TMeP)Ni	3.6	2.0	2.7
(TEtP)Ni	3.4	2.9	2.7
(TPrP)Ni	2.4	3.7	2.7
((*p*-Et_2N)TPP)Ni	1.7	4.4	2.7
(TMeC)Ni	2.0	3.3	3.4

[a] Reaction partially overlaps with first oxidation.

TBAP was carried out for the single reduction as well as for both oxidations of (TMeC)Ni, and the resulting spectra are shown in Figure 7. When the potential was set at −1.50 V for reduction (Figure 7a), both the Soret peak and the peak at 617 nm decreased significantly. This is similar to the changes for anion radical formation with the other complexes in this study. When the potential was set at 0.8 V for the first oxidation (Figure 7b), the peak at 617 nm disappeared and two new peaks occurred at 539 and 754 nm. The latter peak is the characteristic peak of a cation radical. The ESR spectrum taken of this oxidation product displayed an isotropic signal at $g = 2.005$ (295 K) or 2.004 (77 K), confirming the formation of $[(TMeC)Ni^{II}]^+\cdot$. When the second electron was removed, this ESR signal disappeared. The spectrum of this doubly oxidized product is shown in Figure 7c and looks similar to those of $[(TPP)Zn]^{2+}$ and $[(OEP)Mg]^{2+}$ [16] as well as to those of other nickel dications in this study. Therefore, the mechanism for the redox reactions of (TMeC)Ni can be described as shown in Scheme II.

Solvent Effects on Redox Potentials. Half-wave potentials for both oxidation and reduction of (TPP)Ni and (TPrP)Ni were measured in up to 11 different nonaqueous solvents. These results are summarized in Tables IV and V. The solvents in these tables are listed in terms of increasing bonding ability, which is roughly correlated with the Gutmann donor number.[25] It is known from the literature that ((*p*-X)TPP)Ni can form bis(piperidine) adducts with extremely small formation constants.[26] These low formation constants suggest that most of the investigated solvents should not bind to the neutral Ni(II) complexes. Nothing is known, however, regarding the binding characteristics of the oxidized or reduced Ni complexes. If binding did occur, one might therefore observe a positive or negative shift of potential, as was reported in studies of ligand binding by other cation and anion radicals.[27,28]

Very little or no solvent effect was observed for the electrode reactions of Ni(II) porphyrins. Values of $E_{1/2}$ (Tables IV and V) (corrected for liquid junction potential) were virtually identical for each reaction in all solvents except for the first oxidation in py and possibly DMF and Me_2SO. In these three solvents a negative shift of the first oxidation potential was observed such that in py the oxidations of (TPP)Ni and (TPrP)Ni were at 0.69 and 0.55 V vs. SCE, respectively. When corrected for liquid junction potential, this amounts to a negative shift of 330–400 mV from the nonbonding solvents and strongly suggests formation of a mono- or bis(pyridine) adduct for $[(TPP)Ni]^+$ and $[(TPrP)Ni]^+$. However, attempts to identify the exact stoichiometry of these oxidized complexes proved unsuccessful due to an instability of the products in pyridine on the longer time scale required for controlled-potential electrolysis.

Electron-Transfer Rate Constants. Heterogeneous electron-transfer rate constants for all three reactions were measured by cyclic voltammetry and are summarized in Table VI. All of the values are similar and fall within the range of (2–4) $\times 10^{-2}$ cm/s. These values are consistent with those of other metalloporphyrin ring oxidations or reductions[29,30] and are about 1 order of magnitude faster than that of Fc^+/Fc in the same solvent system.[31]

In some cases involving metalloporphyrins there is a difference in heterogeneous rate constants between a metal-centered reaction and a porphyrin-ring-centered reaction.[29,30] This does not appear to be the case in this present study, where

(25) Gutmann, V. "The Donor-Acceptor Approach to Molecular Interactions"; Plenum Press: New York, 1978.
(26) Walker, F. A.; Hui, E.; Walker, J. M. *J. Am. Chem. Soc.* **1975**, *97*, 2390.
(27) Kadish, K. M.; Shiue, L. R.; Rhodes, R. K.; Bottomley, L. A. *Inorg. Chem.* **1981**, *20*, 1274.
(28) Kadish, K. M.; Shiue, L. R. *Inorg. Chem.* **1982**, *21*, 3623.
(29) Kadish, K. M.; Davis, D. G. *Ann. N.Y. Acad. Sci.* **1973**, *206*, 495.
(30) Kadish, K. M.; Morrison, M. M.; Constant, L. A.; Dickens, L.; Davis, D. G. *J. Am. Chem. Soc.* **1976**, *98*, 8387.
(31) Kadish, K. M.; Su, C. H. *J. Am. Chem. Soc.* **1983**, *105*, 177.

all of the second oxidations (one of which is metal centered) have an identical rate constant of 2.7×10^{-2} cm/s. It is interesting to note from Table VI that a correlation appears to exist between the porphyrin ring basicity of the first six complexes and the magnitude of the rates of both the first oxidation and the first reduction. In the former case the rates monotonically increase with increasing basicity while, in the latter case, a decrease in rates is observed. However, the differences are very small, and if these are taken as a whole, one may say that all of the rate constants are virtually identical.

Summary. In conclusion, we have shown that nickel tetraalkylporphyrins and chlorins may be oxidized by two oxidation steps or reduced in a single electron-transfer step similar to the case for (TPP)Ni. It was found that three different mechanisms can occur for oxidations of the different porphyrin complexes. In contrast, only one electrode mechanism governs the reductions.

There is a dramatic shift in the first oxidation potential when one goes from (TPP)Ni, to (TRP)Ni, and then to (TMeC)Ni. A similar 200–210 mV negative shift in potentials is found on going from other metalloporphyrin to metallochlorin systems and can easily be rationalized by the differing energies of the HOMO's and the LUMO's (which have a change in symmetry from D_{4h} to C_{2v}), as well as by a reduction in the total aromatic stabilization of the chlorin relative to the porphyrin complex. It is more difficult, however, to explain the 200-mV negative shift in potential for the three (TRP)Ni^{II} complexes with respect to (TPP)Ni^{II}. The fact that there is no intramolecular electron transfer producing nickel(III) with the tetraalkylporphyrins may indicate that there is an additional stabilization mechanism that is operative. Aggregation has been found in solutions of (TMeC)Ni^{II},[7] and the structure of the conducting (TMeP)Ni^{III}I system indicates that these porphyrins can stack, thus enabling intermolecular interactions to take place. The fact that (TEtP)Ni^{II}, (TPrP)Ni^{II}, and (TMeC)Ni^{II} do not form aggregates might be explained on the basis of steric factors.

Acknowledgment. The support of the National Science Foundation (Grant CHE 8215507) is gratefully acknowledged.

Registry No. ((*p*-Cl)TPP)Ni, 57774-14-8; [((*p*-Cl)TPP)Ni]$^-$·, 88669-53-8; [((*p*-Cl)TPP)Ni]$^+$·, 88669-49-2; [((*p*-Cl)TPP)Ni]$^{2+}$, 88669-58-3; (TPP)Ni, 14172-92-0; [(TPP)Ni]$^-$·, 88669-50-5; [(TPP)Ni]$^+$·, 29484-62-6; [(TPP)Ni]$^{2+}$, 57208-12-5; (TMeP)Ni, 67067-51-0; [(TMeP)Ni]$^-$·, 88669-54-9; [(TMeP)Ni]$^+$·, 78965-41-0; [(TMeP)Ni]$^{2+}$, 88669-59-4; (TEtP)Ni, 75706-99-9; [(TEtP)Ni]$^-$·, 88669-55-0; [(TEtP)Ni]$^+$·, 88669-51-6; [(TEtP)Ni]$^{2+}$, 88669-60-7; (TPrP)Ni, 15245-21-3; [(TPrP)Ni]$^-$·, 88669-56-1; [(TPrP)Ni]$^+$·, 88703-06-4; [(TPrP)Ni]$^{2+}$, 88669-61-8; ((*p*-Et_2N)TPP)Ni, 88669-48-1; [((*p*-Et_2N)TPP)Ni]$^-$·, 88669-57-2; [((*p*-Et_2N)TPP)Ni]$^+$·, 88669-52-7; [((*p*-Et_2N)TPP)Ni]$^{2+}$, 88669-62-9; (TMeC)Ni, 75758-44-0; [(TMeC)Ni]$^-$·, 88685-58-9; [(TMeC)Ni]$^+$·, 88685-57-8; [(TMeC)Ni]$^{2+}$, 88685-59-0; TBAP, 1923-70-2; TBA(PF_6), 3109-63-5.

Contribution from the Department of Chemistry, Kent State University, Kent, Ohio 44242

Electron Transfer. 67. Reductions of Hydroxylamine Derivatives by Vitamin B_{12s} (Cob(I)alamin)[1]

P. N. BALASUBRAMANIAN and E. S. GOULD*

Received July 5, 1983

Vitamin B_{12s} (cob(I)alamin), the Co(I) derivative of vitamin B_{12}, reduces substituted hydroxylamines to the corresponding amines. Specific rates for the reductions of nine alkylated hydroxylamines and hydroxylaminesulfonic acids have been measured and their acid dependencies, in the range 0.01–0.11 M H^+, examined. Reactions of the alkylated hydroxylamines, and that of NH_3OH^+ itself, proceed at rates independent of [H^+], indicating that partition of B_{12s} into protonation levels is not significant in our systems. When rates proportional to [H^+] are observed, as in the reductions of NO_3^- and $HON(SO_3)_2^{2-}$, protonation of the oxidant appears to be occurring. Reduction of NH_3OH^+ to NH_4^+ is considerably slower than that of NO_3^- to NH_4^+ under corresponding conditions, indicating the NH_3OH^+ is not an intermediate in the latter conversion. The 2:1 stoichiometry of the reactions at hand is not altered by additions of alcohols (which have previously shown to divert NH_2· radicals), implying that these reductions, unlike the Cr(II)–NH_3OH^+ reaction, are heterolytic. It is proposed that these reactions proceed via nucleophilic substitution by Co(I), followed by rapid Co(III)–Co(I) comproportionation. The observed kinetic patterns suggest that initial attack occurs predominantly at oxygen for N-alkylated hydroxylamines and *N*-sulfonic acids, but at nitrogen for O-alkylated hydroxylamines and NH_2OSO_3H. The 4e reduction of acetophenone oxime by B_{12s} yields both $C_6H_5CH(CH_3)NH_2$ and $C_6H_5CH(CH_3)OH$. The amine almost certainly arises via initial attack at the C=N double bond of the protonated oxime, whereas the carbinol probably results from substitution at oxygen. Because of competing hydrolysis of the oxime in the medium used, we cannot estimate the relative importance of the two reductive paths.

A sufficient number of redox studies[2] involving vitamin B_{12s}, the cobalt(I) derivative of vitamin B_{12}, have been carried out to demonstrate that this species is a powerful and versatile reductant. We have reported[3] that cob(I)alamin reduces nitrate rapidly and cleanly to NH_4^+ at pH 1.5–2.5, that the overall rate of this net transfer of eight electrons is determined by the initial step, and that the reduction of HNO_2 under the same conditions is, as expected, more rapid than that of NO_3^-. The hydroxylammonium ion, NH_3OH^+, in which the oxidation number of nitrogen is −1, may be considered a logical intermediate in the overall conversion to NH_4^+. If so, NH_3OH^+ should likewise be reduced more rapidly by B_{12s} than is NO_3^-. We find, on the contrary, that it is reduced more slowly and, further, that its reduction is accelerated by N-methylation.

(1) Support of this work by the National Science Foundation (Grant No. 8022881) is gratefully acknowledged.

(2) See, for example: (a) Lexa, D.; Saveant, J.-M. *J. Am. Chem. Soc.* **1976**, *98*, 2652. (b) Itabashi, E.; Parekh, H. V.; Mark, H. B., Jr. *Anal. Lett.* **1978**, *B11*, 515. (c) Kaufmann, E. J.; Espenson, J. H. *J. Am. Chem. Soc.* **1977**, *99*, 7051. (d) Ryan, D. A.; Espenson, J. H.; Meyerstein, D.; Mulac, W. A. *Inorg. Chem.* **1978**, *17*, 3725. (e) Espenson, J. H.; Gjerde, H. B. *Ibid.* **1980**, *19*, 3549. (f) Banks, R. G. S.; Henderson, R. J.; Pratt, J. M. *J. Chem. Soc. A* **1968**, 2886.

(3) Balasubramanian, P. N.; Gould, E. S. *Inorg. Chem.* **1983**, *22*, 2635.

0020-1669/84/1323-0824$01.50/0